Injury 54 (2023) 110777

Contents lists available at ScienceDirect

Injury

journal homepage: www.elsevier.com/locate/injury

A new option for bone regeneration: a rapid methodology for cellularization of allograft with human bone marrow stromal cells with in vivo bone-forming potential☆

Leonardo Rosa da Rocha [a,*], Rhayra Braga Dias [b], Marco Bernardo Cury Fernandes [b], Rafael Prinz [b], Thiago Penna Eirado [b], Isabela de Souza Costa [b], Mauricio J. Monteiro [c], Cristiane Evelise Ribeiro da Silva [d], Claudio Teodoro dos Santos [d], Fabricio Fogagnolo [e]

[a] Teaching and Research Division, Instituto Nacional de Traumatologia e Ortopedia Jamil Haddad (INTO), Av. Brasil, 500, Rio de Janeiro, RJ 20940-070, Brazil
[b] Teaching and Research Division, INTO, Av. Brasil, 500, Rio de Janeiro, RJ 20940-070, Brazil
[c] Materials Division, Instituto Nacional de Tecnologia (INT), Av. Venezuela 82, Rio de Janeiro, RJ 20081-312, Brazil
[d] Materials Division, INT, Av. Venezuela 82, Rio de Janeiro, RJ 20081-312, Brazil
[e] Department of Orthopaedics and Anaesthesiology, Ribeirão Preto Medical School, Universidade de São Paulo (USP), Av. Bandeirantes, 3900, São Paulo, SP 14049900, Brazil

ARTICLE INFO

Keywords:
Allografts
Bone marrow stromal cells
Bone regeneration
Bone bioengineering

ABSTRACT

The treatment of severe musculoskeletal injuries, such as loss of bone tissue and consolidation disorders, requires bone transplantation, and the success of this bone reconstruction depends on the grafts transplant's osteogenic, osteoconductive, and osteoinductive properties. Although the gold standard is autograft, it is limited by availability, morbidity, and infection risk. Despite their low capacity for osteoinduction and osteogenesis, decellularized bone allografts have been used in the search for alternative therapeutic strategies to improve bone regeneration. Considering that bone marrow stromal cells (BMSCs) are responsible for the maintenance of bone turnover throughout life, we believe that associating BMSCs with allograft could produce a material that is biologically similar to autologous bone graft. For this reason, this study evaluated the osteogenic potential of bone allograft cellularized with BMSCs. First, BMSC was characterized and allograft decellularization was confirmed by histology, scanning electron microscopy, and DNA quantification. Subsequently, the BMSCs and allografts were associated and evaluated for adhesion, proliferation, and *in vitro* and *in vivo* osteogenic potential. We demonstrated that, after 2 hours, BMSCs had already adhered to the surface of allografts and remained viable for 14 days. *In vitro* osteogenic assays indicated increased osteogenic potential of allografts compared with beta-tricalcium phosphate (β-TCP). *In vivo* transplantation assays in immunodeficient mice confirmed the allograft's potential to induce bone formation, with significantly better results than β-TCP. Finally, our results indicate that allograft can provide structural support for BMSC adhesion, offering a favorable microenvironment for cell survival and differentiation and inducing new bone formation. Taken together, our data indicate that this rapid methodology for cellularization of allograft with BMSCs might be a new therapeutic alternative in regenerative medicine and bone bioengineering.

Introduction

Bone grafting is one of the most widely used orthopedic surgical procedures to support bone regeneration in suboptimal conditions, such as delayed healing, nonunion, bone defect, poor bone quality, or insufficient blood supply[1,2]. According to Moore et al., for a bone graft to be considered ideal, it must contain 3 complementary properties: osteogenesis, osteoinduction, and osteoconduction[3]. The graft's biological capacity consists of the sum of these basic biological functions. Autografts are considered biologically ideal[4], with the iliac crest

☆ This paper is part of a supplement supported by AO Trauma Latin America.

* Corresponding author.
E-mail addresses: leonardorocha@me.com (L.R. da Rocha), marcobcury@yahoo.com.br (M.B.C. Fernandes), mauricio.monteiro@int.gov.br (M.J. Monteiro), cristiane.evelise@int.gov.br (C.E.R. da Silva), claudio.santos@int.gov.br (C.T. dos Santos).

https://doi.org/10.1016/j.injury.2023.05.008
Accepted 1 May 2023
Available online 23 December 2023
0020-1383/© 2023 Published by Elsevier Ltd.

being the most common source[5]. However, an additional surgical procedure is required to collect, which can result in complications, such as chronic pain, infection, local sensory loss, and instability of the donor site, which can occur in 8.6 to 30% of patients[6–8]. Furthermore, the amount of material that can be removed from this site is limited[9,10], which is the main problem. On average, the volume of cortical-spongy bone available for collection in the anterior and posterior iliac crest is 16 to 26 cm^3 and 34 cm^3, respectively[11].

In situations where autografts are insufficient or impossible, a widely used alternative is allograft, which currently represents 34% of bone grafts[6,12]. Allografts provide a microstructure to sustain vascularization, bone growth, and remodeling during the incorporation period, maintaining osteoconductive potential[13]. One disadvantage of allografts is that the material must be sterilized and decellularized to minimize the risk of disease transmission and immune reactions[14]. However, these procedures can alter the material's biological and mechanical properties, and significant problems often arise from the devitalized allograft's reduced capacity to incorporate into host bone due to a lack of functional bone forming cells[15,16]. One potential treatment strategy entails isolating bone marrow stromal cells (BMSCs) from the patient, expanding them in culture to form cell sheets, and wrapping these sheets on devitalized allografts as a tissue-engineered periosteum prior to transplantation[17].

After many years of evaluating their potential and characterization, today we know that the BMSCs are a set of highly heterogeneous cells isolated from stromal bone marrow that contain both multipotent cells (currently called "skeletal stem cells"), progenitors in different stages of differentiation, and terminally differentiated cells[17–19]. BMSCs are a candidate for bone regeneration therapy due to their unique biological properties, such as innate osteogenicity and the lifelong promotion of bone mass replacement[20]. Thus, we hypothesized that associating allograft with BMSCs could produce a material that is biologically similar to autologous graft, mimicking bone tissue's microenvironment and facilitating the bone neoformation process. In the present study, we analyzed the *in vitro* and *in vivo* osteogenic potential of allograft associated with BMSCs.

Materials and methods

Study design

This study involved *in vitro* and *in vivo* experimental research. The study design, the procedures used for its execution, and the sample collection were approved by the institutional ethics committee (no. 21778619.9.0000.5273).

Sample donor eligibility criteria

For this study, adults aged > 18 years of both sexes undergoing surgery for total hip replacement between February 2020 and January 2021 were invited to donate the discarded acetabular bone/marrow. After providing written informed consent to donate the samples, a brief questionnaire was applied to assess previously diagnosed comorbidities and the risk of blood-borne infections. Exclusion criteria are described in Supplemental table 1.

Sample collection and processing

Acetabular bone fragments were collected and processed immediately after harvesting or after a maximum of 12 hours of storage at 2-8°C in α-minimum essential medium (α-MEM, LGC Biotechnology, São Paulo, SP, Brazil) supplemented with 20% fetal bovine serum (FBS, Gibco/Thermo Fisher, Waltham, MA, USA)[21].

Preparation of bone marrow cell suspensions

The complete protocol has been described in previous publications by this group[22,23]. In brief, for bone marrow cellular dissociation, the bone fragments underwent vigorous mechanical homogenization with phosphate-buffered saline (PBS, Amresco, Solon, OH, USA). The collected marrow suspension was centrifuged at 300 ×g for 5 minutes. The pelleted cells were resuspended in α-MEM supplemented with 20% FBS. To determine the total number of nucleated cells obtained, an aliquot of the marrow suspension was diluted in an appropriate amount of 2% glacial acetic acid for red blood cell lysis, followed by loading in a modified Neubauer chamber for cell counting.

BMSC isolation and in vitro expansion

The complete protocol for BMSC isolation and expansion has been described in previous publications by this group[22,23]. In brief, the mononucleated cells isolated from the samples were subsequently resuspended at a density of $4 \times 10^4/cm^2$ in 10 mL of α-MEM supplemented with 20% FBS and plated in T-75 flasks (Corning). After plating, the cells were allowed to adhere for 3 days in a humidified atmosphere of 5% CO_2 at 37°C incubator. Afterwards, the nonadherent cells were removed, the adherent cells were washed 3 times with PBS, and the medium was changed. Thereafter, the adherent cells were allowed to proliferate for 11 additional days. The cells obtained in the isolation phase were submitted to 2 cycles of *in vitro* expansion (passages) (Supplemental figure 1).

Colony-forming efficiency assay

The frequency of stromal progenitors in the marrow suspension samples was determined through a colony-forming efficiency assay. A total of 2.0×10^5 mononucleated cells from the suspension were seeded in 25 cm^2 culture flasks, with 5 mL of α-MEM supplemented with 20% FBS and incubated at 37°C and 5% CO_2 for 3 days for cell adhesion. The nonadherent hematopoietic cells were then removed, adherent cells were washed with PBS, and the medium was changed. The cultures were maintained for another 11 days, after which the colonies were fixed with 4% paraformaldehyde (MilliporeSigma, Burlington, MA, USA) and stained with 1% crystal violet (MilliporeSigma). Colony forming efficiency was expressed as mean colony number to 100,000 plated bone marrow nucleated cells. Only colonies > 50 cells were counted[17,24].

Immunophenotyping by flow cytometry

At the end of passage 3, the cells were subjected to immunophenotypic characterization. To this end, a total of 1.0×10^6 BMSCs were incubated per tube for 30 minutes in the dark at room temperature with the following fluorochrome-conjugated primary antibodies: anti-CD90-Percp-Cy5.5, anti-CD73-APC, anti- CD105-FITC, anti-CD146-PE (all from BioLegend, San Diego, CA, USA), anti-CD14-FITC (Immunostep, Salamanca, Spain), anti-CD34-FITC, anti-CD45-Percp-Cy5.5 (both from Agilent Dako, Santa Clara, CA, USA), and anti-CD11b-PE (Santa Cruz Biotechnology, Dallas, TX, USA). The isotype controls were IgG2A-FITC, IgG1A-APC, IgG1A-Percp-Cy5.5, IgG1-PE, IgG1-FITC, and IgG2A-PE (all from Santa Cruz Biotechnology). The cells were then washed with FACS buffer and resuspended in 300 µL buffer for acquisition with a Accuri flow cytometer (BD, Franklin Lakes, NJ, USA). The data were analyzed in FlowJo v10 (BD)[25].

In vitro adipogenic and osteogenic differentiation assays

BMSCs were plated at a density of 2.0×10^4 cells/cm^2 in triplicate in α-MEM supplemented with 20% FBS and allowed to grow until 100% confluence was reached. For osteogenic differentiation, the cells were induced by incubation with α-MEM containing 10 mM

β-glycerophosphate, 5 μg/mL ascorbic acid 2-phosphate, and 10^{-6} M dexamethasone (all from MilliporeSigma). After 21 days, the cells were fixed in 4% paraformaldehyde for 10 minutes at room temperature and stained with Von Kossa[17].

For adipogenic differentiation, the cells were incubated with α-MEM containing 0.5 mM isobutylmethylxanthine, 200 mM indomethacin, 10^{-6} M dexamethasone (all from MilliporeSigma), and 10 mM insulin (Humulin, Lilly, São Paulo, SP, Brazil) supplemented with 20% FBS for 21 days. To confirm the lipidic composition of the cell vacuoles, BMSCs were fixed in 4% paraformaldehyde for 15 minutes at room temperature and incubated with 0.5% Oil red O solution (MilliporeSigma)[17].

In vitro chondrogenic differentiation assay

BMSCs were resuspended in α-MEM supplemented with 20% FBS at a density of 1.0×10^6 cells/mL. One 10 μL drop of this cell suspension was placed in each well in a U-shaped 96-well plate, which was incubated at 37°C in 5% CO_2 for 30 minutes. Then, 100 μL of StemPro chondrogenic medium (Gibco Life Technologies, Grand Island, NY, USA) was added to each well. The medium was changed every 2 days for 21 days. On the 21st day, the culture medium was removed, the wells were washed twice with 100 μL of PBS and the micromasses were fixed in 4% paraformaldehyde solution (MilliporeSigma) for 3 hours at room temperature and stained with alcian blue (MilliporeSigma). The slides were photographed using an EVOS microscope (Thermo Fisher Scientific) [26].

Allograft preparation

The allograft samples were harvested and processed for decellularization by the INTO tissue bank and are in accordance with the criteria for allograft donation of the Brazilian National Health Surveillance Agency Resolution No. 220/2006 and the Brazilian National Transplant System.

For decellularization, the allografts were frozen in a mechanical freezer at −80°C for at least 48 hours and subsequently thawed. Then, with an 8G (152 mm) T-handle Jamshidi bone biopsy needle (BD, Franklin Lakes, NJ, USA), 30 mg cylindrical fragments were extracted. The material was subjected to washing cycles with 10% hydrogen peroxide in a digital ultrasonic cleaner (L100, Schuster, Rio Grande do Sul, Brazil) and immersed in absolute alcohol and 0.9% NaCl saline solution with antibiotic (vancomycin 10 mg/mL) for 5 minutes. After processing, the bone fragments were either stored at −80°C or the quality of decellularization was immediately evaluated through DNA quantification, scanning electron microscopy (SEM), and histology[27] (Fig. 1).

DNA quantification in allografts

The amount of DNA in the sample was assessed to validate the allograft decellularization process. Allograft fragments were incubated with lysis solution from a Wizard Genomic DNA Purification kit (Promega, Madison, WI, USA) in a water bath at 55°C for 12 hours. The next day, magnetic beads were placed in 1.5 mL conical tubes, and the tissue was fragmented using a tissue disruptor (L-Beader 24, Loccus, SP, Brazil) for 5 cycles at 3733 rpm for 40 seconds. After these steps, DNA was extracted using a Wizard Genomic DNA Purification Kit (Promega) according to manufacturer recommendations. The amount of DNA extracted from 30 mg of tissue was quantified in a NanoDrop spectrophotometer (Thermo Fisher Scientific). Values were expressed in ng/μL[14].

Cellularization of scaffolds with BMSCs

We incubated 1.0×10^6 BMSCs with 30 mg of scaffold, ie, 30 mg of allograft or beta-tricalcium phosphate (β-TCP), under agitation at 250 rpm in an orbital shaker table for 2 hours (Tecnal, São Paulo, SP, Brazil). After that time, part of the material was used for evaluation of cell adhesion by SEM, another part was kept in culture for up to 21 days for proliferation and differentiation assays, and the remaining samples were sent to the *in vivo* differentiation assay[23].

The β-TCP (ChronOS, Synthes, Oberdorf, Switzerland), a synthetic bone graft substitute with 60% porosity and pores ranging from 100 to 500 μm, was used as a control group[28]. Using an 8G (152 mm) T-handle Jamshidi bone biopsy needle (BD), 30 mg cylindrical fragments were extracted (Fig. 1).

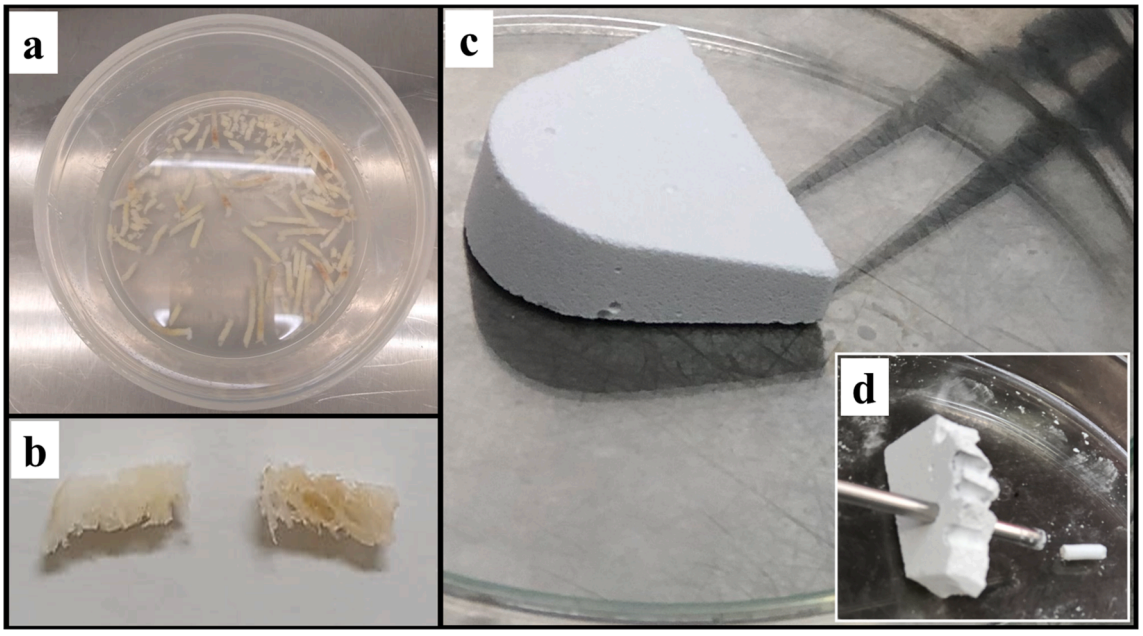


Fig. 1. Bone allograft and beta-tricalcium phosphate preparation. Macroscopic view of cylindrical allograft fragments (a,b) and the β-TCP (c,d). Example of extraction of 30 mg cylindrical fragments using a bone biopsy needle (d).

Scanning electron microscopy

The scaffold (ie, 30 mg of allograft or β-TCP) was fixed with 2.5% glutaraldehyde (Merck, Darmstadt, Germany) in 0.1 M sodium cacodylate buffer for 2 hours, post-fixed for 30 minutes with a 1% osmium tetroxide solution in sufficient quantity to cover the sample. The material was then dehydrated in a series of alcohol gradients (30%, 50%, 70%, 90%, and 100%). Each concentration was used twice for 15 min. At the end of dehydration, the samples were immersed in an alcohol solution of hexamethyldisilane (MilliporeSigma), 1:1 (v/v), for 30 minutes, followed by a further 30 minutes of incubation with pure hexamethyldisilane solution. The samples were then kept for 12 hours in Fume hood for drying, and the metallization process was performed with a nanometric layer of gold. Gold was deposited using a metallizer with the ionic deposition parameters set as follows: temperature in the metallization chamber of 25°C, current of 40 mA, voltage of 2 kV, and deposition time of 140 seconds, resulting in a gold film on the surface of the granulated biomaterial of 30 nm.

Acquisition and analysis were performed at a voltage of 15 kV in low vacuum mode on a Quanta 400 SEM (Thermo Fisher) at the National Institute of Technology's Center for Characterization in Nanotechnology (Rio de Janeiro, RJ, Brazil). SEM was performed before cellularization to characterize the microstructure of the scaffolds and to evaluate allograft preparation quality. After cellularization with BMSCs, SEM was used to evaluate the cells' morphology and adhesion capacity in allograft and β-TCP.

In vitro cell viability and proliferation assay

After cellularizing the scaffolds with BMSCs, the implants were cultured with α-MEM with 20% FBS at 37°C, 5% CO_2 for 14 days; cell viability and its proliferation were analyzed with a Cell Counting Kit-8 (CCK-8, Merck). After culturing the cells for 1, 3, 6, 10, and 14 days, 10 μL CCK-8 solution was added to each well and they were incubated for 4 hours at 37°C. The absorbance of each well was then measured in a detector at 450 nm using a Glomax spectrophotometer (Promega), with the results expressed as optical density. To detect differences in cellular metabolic activity, 3 groups were formed: the ALO^{BMSC} group (BMSCs + allograft); the TCP^{BMSC} group (BMSCs + β-TCP); and the control group (BMSCs adhered to the culture plate without scaffold)[29].

In vitro assay of osteogenic differentiation capacity

After cellularizing the scaffolds with BMSCs, the implants were cultured in osteogenic differentiation medium for 21 days. To evaluate differentiation in the early phase, alkaline phosphatase activity was measured at 7 and 14 days of cultivation in both groups (ALO^{BMSC} and $\beta\text{-}TCP^{BMSC}$) according to manufacturer specifications (Alkaline Phosphatase Diethanolamine Activity, Merck). On the 21st day, the deposition capacity of the mineralized matrix was determined, and the scaffolds were fixed with 500 μL of 4% paraformaldehyde solution for 3 hours and stained with alizarin red S. To quantify the deposition of the mineralized matrix, alizarin red was eluted with 10% acetic acid and incubated at 85°C for 10 minutes. The material was then kept on ice for 5 minutes and centrifuged at 20000 × g for 15 minutes. The acid was then neutralized with 10% ammonium hydroxide and the absorbance was detected using a Glomax spectrophotometer (Promega) at a wavelength range of 405 nm. The results were expressed as optical density[30,31].

In vivo evaluation of the osteogenic potential of cellularized graft

A total of 12 eight-week-old male and female immunodeficient mice (C57BL/6. Cg-Foxn1nu, INTO, Rio de Janeiro, RJ, Brazil) with an average weight of 30 (SD, 5) g were used for animal model experiments [17,18]. Four implants were transplanted per mouse: 2 without the cells (ALO^0 and $\beta\text{-}TCP^0$) and 2 with the cells (ALO^{BMSC} and $\beta\text{-}TCP^{BMSC}$) (Supplemental figure 2). The surgical procedures were performed under general anesthesia via inhalation with isoflurane (anesthetic plane induction 5%, intraoperative 2%). After surgical asepsis, a longitudinal incision of approximately 20 mm was made in the mouse's flank, forming subcutaneous pockets in paravertebral regions. The subcutaneous layers and skin were then closed in a simple pattern using 5/0 Ethilon nylon sutures (Ethicon, Raritan, Nova Jersey, USA). Postoperatively, the animals received analgesia with tramadol hydrochloride, 12 mg/kg (Farmace, Barbalha, Ceara, Brazil), subcutaneously twice a day for 2 days. After 12 weeks, the mice were euthanized by inhalation and the implants were harvested. All animal procedures were performed according to Institutional Animal Care and Use Committee guidelines (008/2019).

Histological and histomorphometry analyses

Following the harvesting procedure, the implants were fixed for 24 hours in 4% paraformaldehyde in PBS. For routine histology, the implants were decalcified by incubation in 10% nitric acid (Vetec) for 3 days, processed for paraffin embedding, cut into 5 μm sections using a RM2255 microtome (Leica Biosystems, Wetzlar, Germany), and stained with hematoxylin and eosin and Goldner's trichrome stain (both from ScyTeK, Logan, UT, USA) according to standard protocols. All images from the glass slides were obtained through digital scanning with an Aperio CS2 scanner and Image-Scope software (both from Leica Biosystems). The histomorphometry was performed on whole implant sections using ImageJ software (NIH, Bethesda, MD, USA) with the BoneJ plugin v1.3 (https://bonej.org) according to Malhan's protocol (2018). The total volume of new bone formation for all 4 groups was estimated based on the percentage within the evaluated area[32,33].

Statistical analysis

The values were expressed either individually, as mean (SD) or median, as appropriate. P values ≤ 0.05 were considered significant. The analyses were performed in GraphPad Prism v8.0 (GraphPad, San Diego, CA, USA). Nonparametric Mann-Whitney tests were performed for the CCK-8 data and alkaline phosphatase quantification data. Welch's t-test was used for the alizarin red staining data. The 3 samples were compared using the Kruskal-Wallis test.

Results

Patient and sample characteristics, frequency analysis of fibroblast colony-forming units, and BMSC expansion

Samples were collected from 5 patients (4 male and 1 female) with a mean age of 53 (SD, 17.60) years. The cell expansion process was not performed for 1 sample due to insufficient cells. The number of colonies harvested from each sample ranged from 20.0 to 29.6 fibroblast colony-forming units per 100,000 nucleated cells, with a mean of 22.75 (SD, 4.63) ($p = 0.06$). At the end of the third passage, the mean BMSC yield was 34.25 (SD, 10.99) × 10^6 cells, and cell viability was 94.77% (SD,

Table 1
Patient characteristics, frequency analysis of fibroblast colony-forming units, and BMSC expansion.

Sample	Age (years)	Sex	CFU frequency (10^5)	Viability (%)	Total BMSCs after P3 (10^6)
1	37	M	21	98	50
2	61	F	20.33	95	25
3	74	M	20	93.2	33
4	40	M	29.67	92.9	29
Mean ± SD	53 ± 17.60		22.75 ± 4.63	94.77 ± 2.34	34.25 ± 10.99

F = female; M = male; P3 = third passage; x = no cell expansion; n = 5.

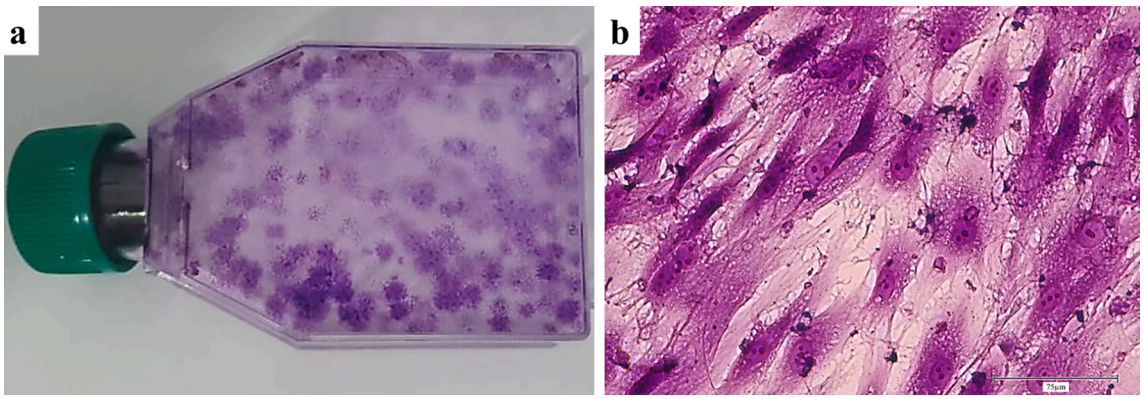


Fig. 2. Frequency analysis of fibroblast colony-forming units. Macroscopic and microscopic representative images of colonies from different samples (a,b). n = 4 and scale bar=75um.

2.34) (Table 1, Fig. 2).

Immunophenotypic characterization and in vitro differentiation of BMSCs

To characterize the cell products, we first assessed the expression of BMSC-related cell surface markers with fluorescence-activated cell sorting. The expanded BMSCs homogeneously expressed > 95% of the classic markers (CD73, CD90, CD105, and CD146) and less than 2% of the hematopoietic lineage markers CD34, CD45, CD14, and CD11b (Fig. 3A and Supplemental table 2). Next, we evaluated their differentiation potential *in vitro* for the adipogenic, osteogenic, and chondrogenic pathways. The induced BMSCs could differentiate into osteoblasts, adipocytes, and chondrocytes, as shown by the deposition of mineralized nodules (a characteristic phenotype of osteoblasts) (Fig. 3D), intracellular lipid accumulation (a characteristic of adipocytes) (Fig. 3C), and the formation of a matrix rich in proteoglycans, (a characteristic of chondrocytes) (Fig. 3E). All in all, these results demonstrate the successful isolation of cells and confirm their nature as BMSCs.

Quality assessment of allograft decellularization

To assess the quality of the allograft decellularization process, we performed DNA quantification, histology, and SEM. Spectrophotometry quantification indicated a low amount of DNA in the allograft, on average 23.25 (SD, 5) ng of DNA for every 30 mg of tissue. The histological analysis identified no viable cells or osteocytes in lacunae (Fig. 4A). In SEM analysis, we observed preserved tissue microarchitecture and a lack of cells deposited on the bone surface (Fig. 4B and 4C).

Evaluation of BMSC adhesion and proliferation in the allograft

In evaluation of the cellularization process, SEM images revealed that the BMSCs had already adhered to the surface of both materials after 2 hours. For 14 days after adhesion, we evaluated the proliferation capacity of BMSCs adhered to the allograft or β-TCP. We compared the proliferation curve of the BMSCs with the CCK-8 assay, finding that exponential growth did not occur in the population that adhered to the scaffolds. However, BMSCs that adhered to the allograft and β-TCP remained metabolically active, that is, viable for 14 days ($p = 0.07$) (Fig. 5).

In vitro evaluation of induced osteogenic differentiation

To assess the allograft's ability to induce osteogenic differentiation, in the initial period we quantified alkaline phosphatase activity. On the seventh day after osteogenic induction, the BMSCs showed no enzymatic activity in either group, while on the 14th day, enzyme activity peaked in the allograft group. Comparing both groups, we observed more enzymatic activity in osteoinduced cells in allograft ($p = 0.08$) (Fig. 6A). In the second step, we evaluated effective deposition of the osteogenic matrix by alizarin red staining. When comparing the groups at 14 and 21 days, there was a progressive change in the shade of red, indicating an increased degree of mineralization in BMSCs that adhered to the allograft or β-TCP (Fig. 6B). On the 21st day, more significant mineralization was observed in the BMSC cultures from the allograft group ($p = 0.03$) (Fig. 6C).

Evaluation of the osteogenic potential of allograft cellularized with BMSCs (in vivo assay)

Twelve weeks after the subcutaneous transplant, we evaluated new bone formation. In the ALO^{BMSC} group, it was possible to identify the division between old and new bone, a cementing line. The old bone had been formed with observable lamellae, guided by collagen fibers and an absence of cells, and the new bone which consisted of a region with an amorphous aspect, no defined fiber organization, and osteocytes still in the maturation phase (Fig. 7A and 7C). The histological differences in newly formed bone between groups are more evident in comparison with the tissue structure of the ALO^{0} group, in which there was only old decellularized bone (Fig. 7E). Comparing the $\beta\text{-TCP}^{0}$ group with the $\beta\text{-TCP}^{BMSC}$ group, bone neoformation around the crystal granules and osteocytes in lacunae were observed only in the $\beta\text{-TCP}^{BMSC}$ group (Fig. 7B and 7F). In quantitative evaluation, a higher percentage of new bone formation was observed in the ALO^{BMSC} group (27.62% [SD, 6.42%]) than the $\beta\text{-TCP}^{BMSC}$ group (18.11% [SD, 6.30%]) ($p = 0.01$) (Fig. 7G).

Discussion

Despite advances in orthopedic bioengineering, new treatment options are needed to improve fracture healing. In this context, previous studies have shown that allografts seeded with BMSCs accelerate the healing of critically-sized bone defects in rats[34]. However, in humans, little is known about the advantages of associating BMSCs with allografts or whether they are a viable option for treating bone defects.

The protocols used to isolate and expand BMSCs in this study were based on the previous experience of our group[22,23] and international groups[18,21]. Regarding *in vitro* expansion, some methodologies employ 3 to 44 passages expansion[35–38]. Studies whose cell samples underwent an expansion process with 3 passages[39–41], 4 passages [42,43], and 5 passages[44] maintained expression of surface markers and fibroblastoid morphology. However, prolonged cultivation of BMSCs delays proliferation and leads to senescence[45,46] and loss of multipotentiality[47–50]. In fact, in the protocol established by our group, the BMSCs homogeneously expressed stromal cell surface

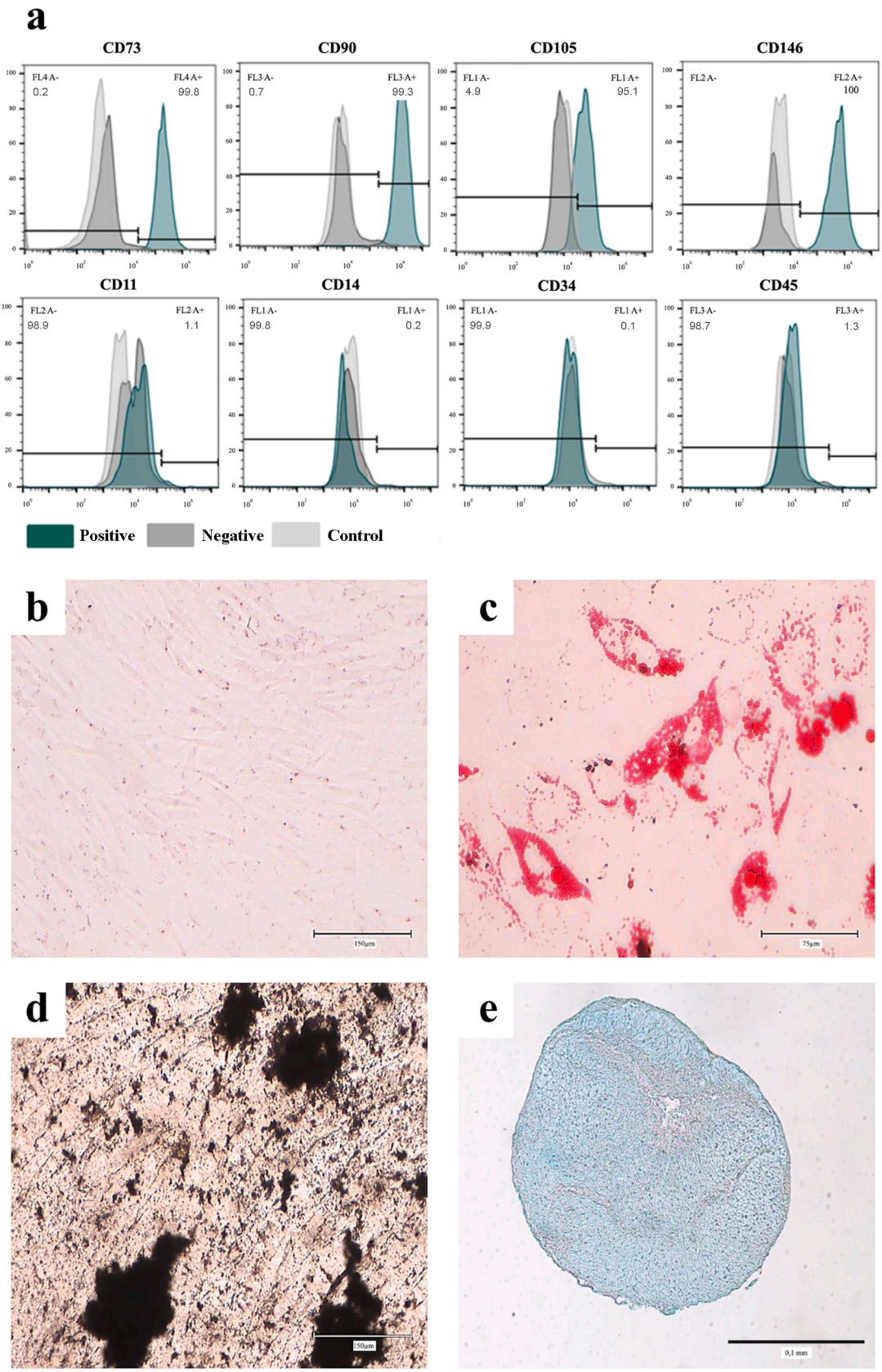


Fig. 3. Immunophenotypic characterization and *in vitro* differentiation of BMSCs. Flow cytometry histograms showing the percentages of cells expressing CD90, CD73, CD105, CD146, CD11b, CD14, CD34 and CD45 (green) compared to the corresponding isotypes (dark gray) and unlabeled cells (light gray) (a). Representative images of (b) a noninduced BMSC, (c) intracellular lipid accumulation stained with Oil Red O, (d) mineralized nodules visualized by Von Kossa staining, and (e) chondrogenic differentiation with alcian blue.

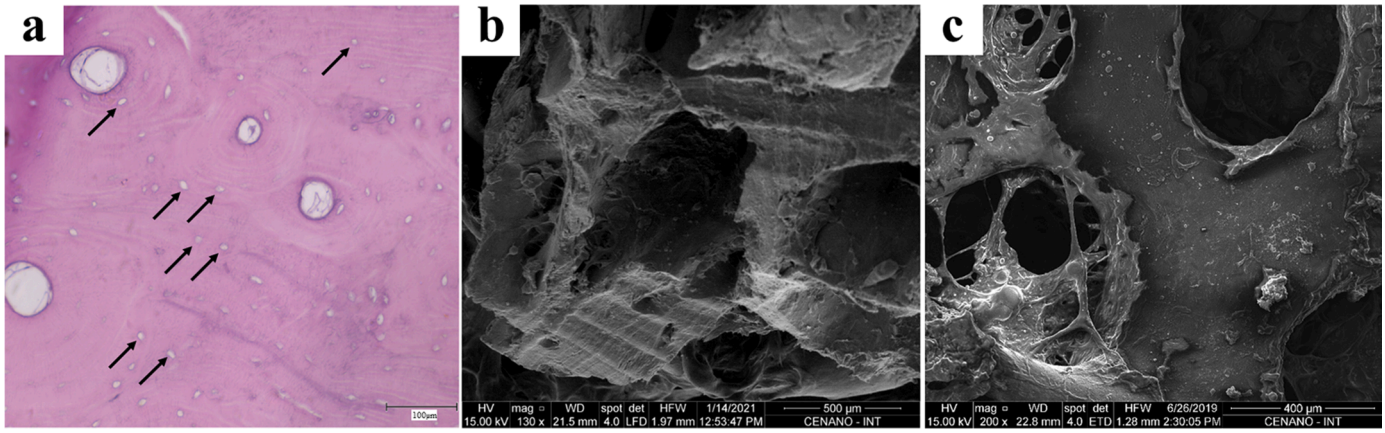


Fig. 4. Quality assessment of allograft decellularization. (a) Histological section of the allograft with H&E staining, black arrows demonstrating lacunae without osteocytes. (b, c) Structural aspects of the allograft on SEM at 130x magnification and at 200x magnification.

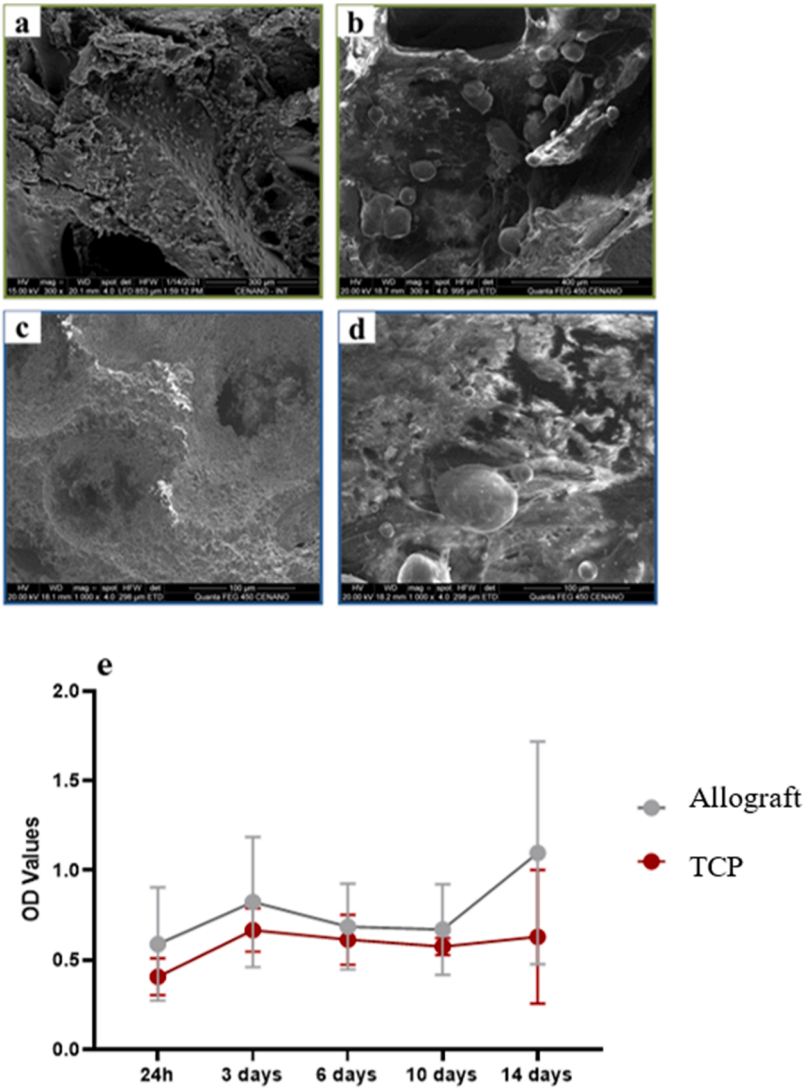


Fig. 5. Evaluation of BMSC adhesion and proliferation in the allograft. SEM showing the BMSCs adhered to the allograft (a,b) and β-TCP (c,d). (e) Evaluation of BMSC proliferation and viability through the CCK-8 assay 14 days after incubation with allograft and β-TCP (n = 4), p=0.07.

markers, such as CD73, CD90, CD105, and CD146. They maintained their ability to differentiate into osteogenic, chondrogenic, and adipogenic lineages, confirming that we generated cells that maintained the phenotypic and functional characteristics of BMSCs as defined by International Society for Cell & Gene Therapy[51].

Associating transplanted BMSCs with biomaterials is one of the most

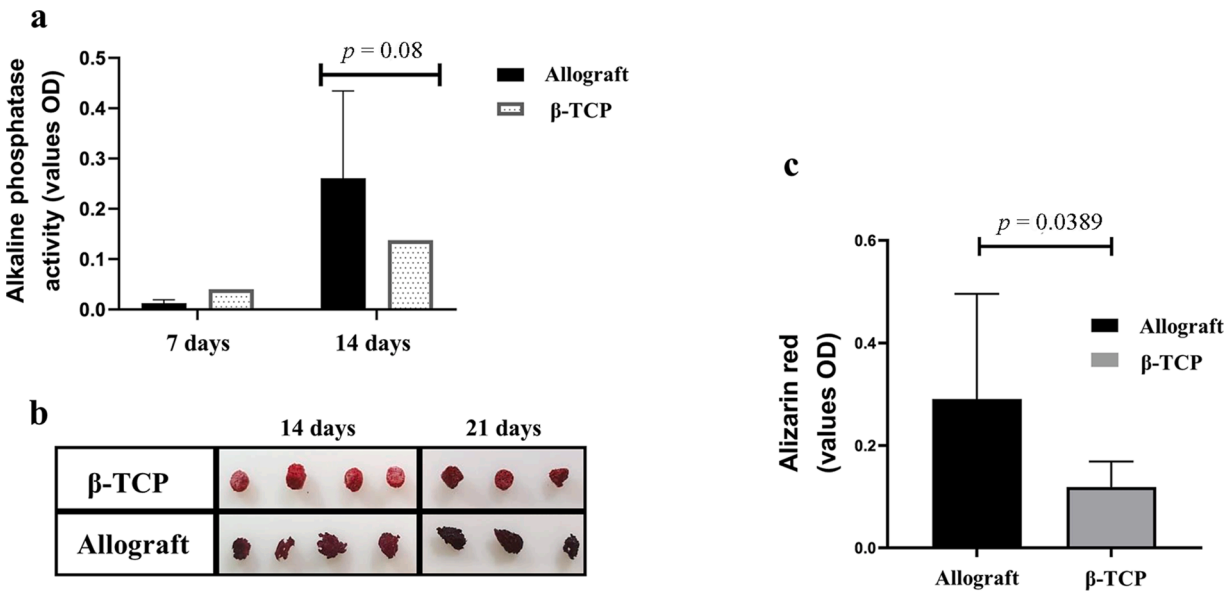


Fig. 6. *In vitro* evaluation of osteogenic differentiation potential. (a) Quantification of alkaline phosphatase activity in groups of BMSCs in the presence of allograft and β-TCP (p = 0.08, Mann-Whitney test). (b) Macroscopic images of allograft and β-TCPs stained with red alizarin on days 14 and 21. (c) Quantification of the extent of *in vitro* osteogenic differentiation on day 21 (p = 0.039, Welch's t-test). Graphs represent mean ± standard deviation; (n=4)

promising strategies for bone reconstruction, providing a niche for differentiating osteoprogenitor cells and guiding new bone formation. In this study, we focused on evaluating allograft as a scaffold for BMSCs due to its ease of access and its biological, structural, and mechanical similarities to autograft[52]. However, residual cellular material within the allograft can contribute to compatibility issues and adverse reactions in hosts[14]. Therefore, validating the allograft decellularization process is a fundamental step in guaranteeing the safety and effectiveness of transplants[53].

In this context, the effectiveness of the tissue cell removal process can be evaluated through several methodologies, such as the hematoxylin and eosin technique, SEM, histological evaluation of nuclear content, and quantification of genetic material[14]. In slides stained with hematoxylin and eosin, the osteocytes in lacunae were eliminated after processing the material. This parameter is the most common one in the literature to indicate tissue devitalization[54,55]. Likewise, nuclear labeling with 4′,6-diamidino-2-phenylindole and SEM is consistent with the hematoxylin and eosin results. It corroborates the hypothesis of successful cell elimination, which has also been observed in decellularization tests in the literature[56].

Regarding DNA quantification, Smith et al. demonstrated that after successive washes, 99.2% of the DNA had been removed, resulting in a final DNA content of 16.9 ng/mg in allograft[57]. Rasch et al. tested 2 different protocols, achieving an average DNA reduction of 99.8%, with a mean value of 40.3 ng/mg in allograft[27]. In these studies and our study, the DNA concentrations of the final product were < 50 ng/mg of tissue, which Crapo et al. considered a parameter for tissue decellularization[14]. Thus, we conclude that the protocol used to decellularize allografts effectively removed residual donor material, which could result in lower immune reactions.

During the second period, we sought to standardize a cellularization method that could be used in clinical trials. A literature search indicated a BMSC coverage rate of 15% in allograft[58] and that 45 to 50% of BMSCs adhered to synthetic scaffold particles after 1 hour of association [59]. Similarly, Mebarki et al. observed that after 3 hours of incubation, 49% of BMSCs had adhered to the allograft, while 28% had adhered to β-TCP[60]. Considering these results and the feasibility of applying this protocol in the surgical center intraoperatively, we determined that 2 hours would be sufficient to associate BMSCs with the allograft. Given the context of cell therapy and bioengineering protocols, the establishment of a protocol that can be adopted within the surgical center, during the intraoperative period, might minimize the risks of contamination and optimize the treatment to be applied to the patient.

Adhesion, viability, and cell proliferation are important initial parameters for evaluating a scaffold's biocompatibility with BMSCs. In *in vitro* assays, we sought to determine whether allograft can provide an adequate microenvironment to maintain the viability of BMSCs and stimulate both the proliferation and differentiation of these cells. We evaluated cellularization efficiency through SEM at 2 different time points, ie, after 2 hours and 14 days, as in other studies[27,61]. Morphological comparison of BMSCs adhered to the external surface of β-TCP and allograft showed a rounded morphology in β-TCP but more fusiform cells with cytoplasmic extensions in allograft, indicating early adhesion and greater efficiency[27,60]. Indeed, the spongy architecture of the allograft appears to induce better adhesion. The high number of closed pores in β-TCP concentrates cells on the outer surface area and may hinder infiltration[62]. We concluded that both scaffold types could provide structural support for BMSC adhesion.

We evaluated cell viability and proliferation in allograft with the CCK-8 test. Qi et al. and Lu et al. used CCK-8 in their *in vitro* experiments, concluding that BMSCs adhered and proliferated on the surface of scaffolds[63,64]. Our results confirm these data, and we observed that the cells remained viable and metabolically active throughout the experiments.

We evaluated the differentiation capacity of BMSCs adhered to allograft by assessing alkaline phosphatase activity, the enzyme responsible for converting organic phosphate into inorganic phosphate, which is essential for mineralized matrix deposition[30]. We also quantified matrix deposition using alizarin red staining[65]. In our study, BMSCs showed slight alkaline phosphatase activity in the first week, with significantly increased expression the following week. However, slightly higher alkaline phosphatase activity was observed in the ALO^{BMSC} group than the $\beta\text{-TCP}^{BMSC}$ group. Our data agree with Mebarki et al.[60], who observed increased osteogenic activity in the first 2 weeks, with higher performance in the allograft group than the β-TCP group.

To confirm that BMSCs associated with allograft induced osteogenesis, we quantified mineralized matrix deposition. Alizarin red forms a chelate complex with deposited calcium and thus can be used as a quantifiable indicator of bone mineralization potential[66]. In this

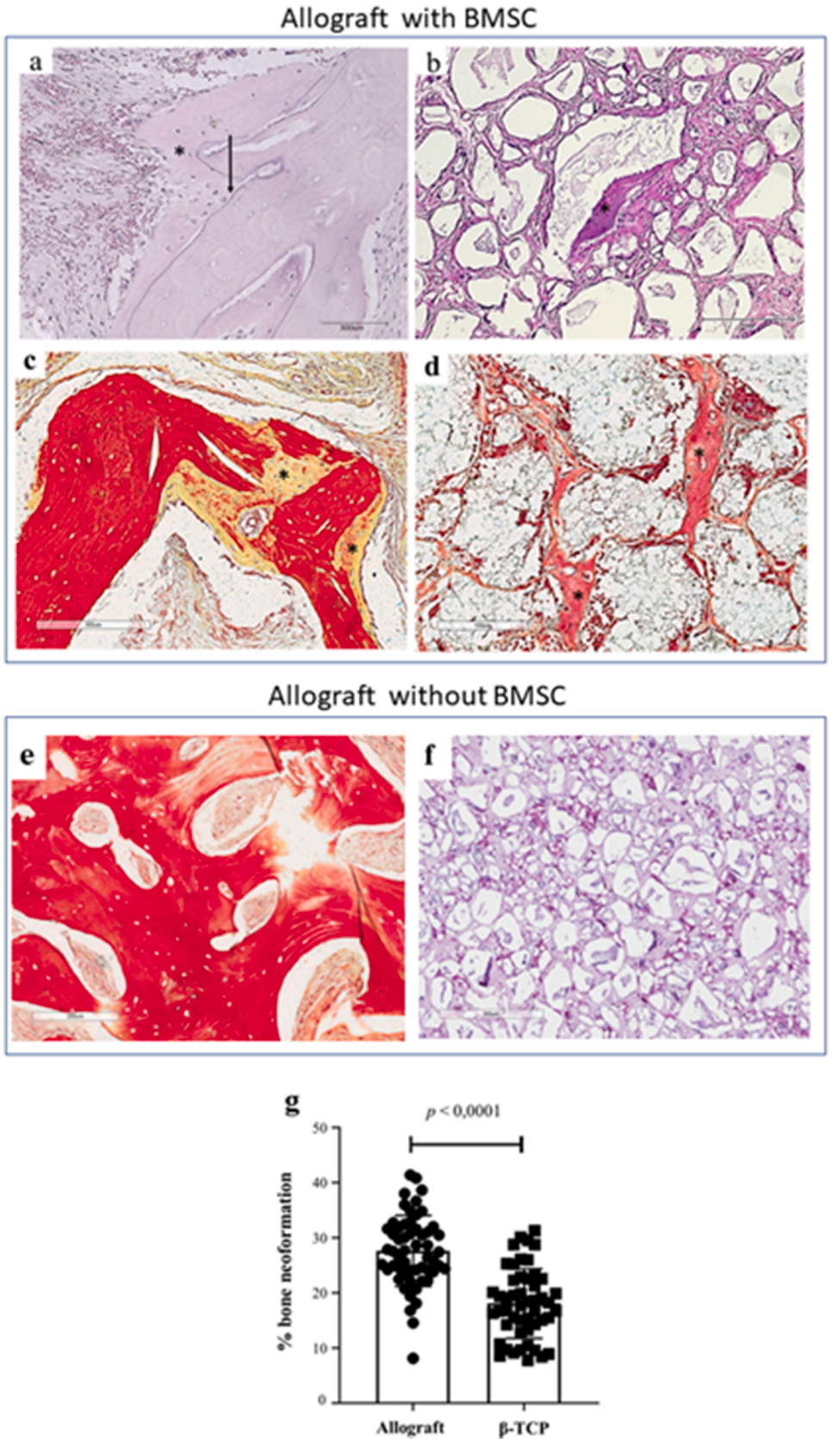


Fig. 7. *In vivo* evaluation of the osteogenic potential of allograft cellularized with BMSCs. Histological images of allograft or β-TCP with and without BMSCs. Arrow = cementing line, which consists of the separation between the allograft and the new bone, (*) Asterisk identifying the area of bone neoformation and heterotopic bone formation. (e) Histomorphometric analysis. $p > 0.0001$, Mann-Whitney test. (a, b, c) H&E stain and (c, d, e) Goldner's trichrome stain.

assay, more effective deposition of extracellular mineralized matrix occurred in the ALO^{BMSC} group than the β-TCP group. In these *in vitro* assays, we proved that allograft can support the adhesion, survival, and differentiation of BMSCs.

Although *in vitro* assays are often used to assess osteogenesis, *in vivo* transplantation is the gold standard to assess osteogenic differentiation [67], since it is considered more representative of the living body, mimicking the complexity of the microenvironment in clinical situations of interest[68]. In the present study, the *in vivo* assay evaluated the osteogenic potential of allograft cellularized with BMSCs, verifying that these cells expanded *in vitro* maintained the ability to differentiate and form bone, as observed in the *in vitro* assays. Quantitatively, we observed that new bone formation was greater in the allograft group than the β-TCP group. In agreement with *in vivo* studies, our results demonstrate that cellularized allografts with mesenchymal progenitors promoted osteogenic differentiation and improved bone neoformation[58,68].

The difficulty in establishing a segmental bone defect model in immunodeficient mice is the main limitation of this study. To address this shortcoming, *in vivo* experiments that effectively assess whether associating BMSCs with allograft can stimulate bone regeneration should be performed to guarantee biological success. Finally, the allograft's potential to induce bone formation *in vivo* with superiority to β-TCP is important evidence that associating BMSCs with allograft appears as a promising strategy for clinical trials in bone bioengineering.

Conclusion

We conclude that allograft can provide structural support for BMSC adhesion, offering a favorable microenvironment for cell survival and differentiation and inducing new bone formation. Taken together, our data indicate that this rapid methodology for cellularization of allograft with BMSCs might be a new therapeutic alternative in regenerative medicine and bone bioengineering.

Supplementary material

Supplemental figure 1. Schematic representation of *in vitro* bone marrow stromal cell isolation and expansion. After bone marrow dissociation from bone spicules, nucleated cells were seeded in T-75 flasks for 14 days (a), followed by expansion for 2 passages (b).

Supplemental figure 2. Schematic representation of *in vivo* evaluation of the osteogenic potential of cellularized graft. Four implants were transplanted per mouse, 2 without the cells (ALO^0 and $\beta\text{-}TCP^0$) and 2 with the cells (ALO^{BMSC} and $\beta\text{-}TCP^{BMSC}$).

Financial disclosure

The study was partially supported by the AO Trauma Latin America Research Office.

Ethical approval

This study involved *in vitro* and *in vivo* experimental research. The study design, the procedures used for its execution, and the sample collection were approved by the INTO ethics committee (n^o 21778619.9.0000.5273).

Declaration of Competing Interest

The authors have no conflicts of interest to disclose.

Supplementary materials

Supplementary material associated with this article can be found, in the online version, at doi:10.1016/j.injury.2023.05.008.

References

[1] Fillingham Y, Jacobs J. Bone grafts and their substitutes. Bone Joint J 2016;98-B:6–9.
[2] Giannoudis PV, Dinopoulos H, Tsiridis E. Bone substitutes: an update. Injury 2005;36(Suppl 3):S20–7.
[3] Moore WR, Graves SE, Bain GI. Synthetic bone graft substitutes. ANZ J Surg 2001;71:354–61.
[4] Sen MK, Miclau T. Autologous iliac crest bone graft: should it still be the gold standard for treating nonunions? Injury 2007;38(Suppl 1):S75–80.
[5] Zigdon-Giladi H, Rudich U, Michaeli Geller G, Evron A. Recent advances in bone regeneration using adult stem cells. World J Stem Cells 2015;7:630–40.
[6] Oryan A, Alidadi S, Moshiri A, Maffulli N. Bone regenerative medicine: classic options, novel strategies, and future directions. J Orthop Surg Res 2014;9:18.
[7] Frohlich KL, Potvin L. Transcending the known in public health practice: the inequality paradox: the population approach and vulnerable populations. Am J Public Health 2008;98:216–21.
[8] Baldwin P, Li DJ, Auston DA, Mir HS, Yoon RS, Koval KJ. Autograft, allograft, and bone graft substitutes: clinical evidence and indications for use in the setting of orthopaedic trauma surgery. J Orthop Trauma 2019;33:203–13.
[9] St John TA, Vaccaro AR, Sah AP, Schaefer M, Berta SC, Albert T, et al. Physical and monetary costs associated with autogenous bone graft harvesting. Am J Orthop (Belle Mead NJ) 2003;32:18–23.
[10] France JC, Schuster JM, Moran K, Dettori JR. Iliac crest bone graft in lumbar fusion: the effectiveness and safety compared with local bone graft, and graft site morbidity comparing a single-incision midline approach with a two-incision traditional approach. Global Spine J 2015;5:195–206.
[11] Kilinc A, Korkmaz IH, Kaymaz I, Kilinc Z, Dayi E, Kantarci A. Comprehensive analysis of the volume of bone for grafting that can be harvested from iliac crest donor sites. Br J Oral Maxillofac Surg 2017;55:803–8.
[12] Zimmermann G, Moghaddam A. Allograft bone matrix versus synthetic bone graft substitutes. Injury 2011;42(Suppl 2):S16–21.
[13] Faldini C, Miscione MT, Acri F, Chehrassan M, Bonomo M, Giannini S. Use of homologous bone graft in the treatment of aseptic forearm nonunion. Musculoskelet Surg 2011;95:31–5.
[14] Crapo PM, Gilbert TW, Badylak SF. An overview of tissue and whole organ decellularization processes. Biomaterials 2011;32:3233–43.
[15] Sohn HS, Oh JK. Review of bone graft and bone substitutes with an emphasis on fracture surgeries. Biomater Res 2019;23:9.
[16] Chatterjea A, Meijer G, van Blitterswijk C, de Boer J. Clinical application of human mesenchymal stromal cells for bone tissue engineering. Stem Cells Int 2010;2010:215625.
[17] Robey PG, Kuznetsov SA, Bianco P, Riminucci M. Bone marrow stromal cell assays: in vitro and in vivo. Methods Mol Biol 2021;2230:379–96.
[18] Robey PG, Kuznetsov SA, Ren J, Klein HG, Sabatino M, Stroncek DF. Generation of clinical grade human bone marrow stromal cells for use in bone regeneration. Bone 2015;70:87–92.
[19] Holzwarth K, Kohler R, Philipsen L, Tokoyoda K, Ladyhina V, Wahlby C, et al. Multiplexed fluorescence microscopy reveals heterogeneity among stromal cells in mouse bone marrow sections. Cytometry A 2018;93:876–88.
[20] Rosset P, Deschaseaux F, Layrolle P. Cell therapy for bone repair. Orthop Traumatol Surg Res 2014;100:S107–12.
[21] Sabatino M, Ren J, David-Ocampo V, England L, McGann M, Tran M, et al. The establishment of a bank of stored clinical bone marrow stromal cell products. J Transl Med 2012;10:23.
[22] Dias RB, Guimaraes JAM, Cury MB, Rocha LR, da Costa ES, Nogueira LP, et al. The manufacture of GMP-grade bone marrow stromal cells with validated in vivo bone-forming potential in an orthopedic clinical center in Brazil. Stem Cells Int 2019;2019:2608482.
[23] Dias RB, Bonfim DC. The Isolation and manufacture of GMP-grade bone marrow stromal cells from bone specimens. Methods Mol Biol 2021;2286:95–105.
[24] Kuznetsov SA, Mankani MH, Bianco P, Robey PG. Enumeration of the colony-forming units-fibroblast from mouse and human bone marrow in normal and pathological conditions. Stem Cell Res 2009;2:83–94.
[25] Rocha LR, Sartore RC, Leal AC, Dias RB, Duarte MEL, Guimaraes JAM, et al. Bone intramedullary reaming grafts the fracture site with CD146(+) skeletal progenitors and downmodulates the inflammatory environment. Injury 2017;48(Suppl 4):S41–SS9.
[26] Nasrabadi D, Rezaeiani S, Eslaminejad MB, Shabani A. Improved protocol for chondrogenic differentiation of bone marrow derived mesenchymal stem cells -effect of PTHrP and FGF-2 on TGFbeta1/BMP2-induced chondrocytes hypertrophy. Stem Cell Rev Rep 2018;14:755–66.
[27] Rasch A, Naujokat H, Wang F, Seekamp A, Fuchs S, Kluter T. Evaluation of bone allograft processing methods: impact on decellularization efficacy, biocompatibility and mesenchymal stem cell functionality. PLoS One 2019;14:e0218404.
[28] Seebach C, Henrich D, Wilhelm K, Barker JH, Marzi I. Endothelial progenitor cells improve directly and indirectly early vascularization of mesenchymal stem cell-driven bone regeneration in a critical bone defect in rats. Cell Transplant 2012;21:1667–77.
[29] Liu D, Nie W, Li D, Wang W, Zheng L, Zhang J, et al. 3D printed PCL/SrHA scaffold for enhanced bone regeneration. Chem Eng J 2019;362:269–79.
[30] Kuehlfluck P, Moghaddam A, Helbig L, Child C, Wildemann B, Schmidmaier G, et al. RIA fractions contain mesenchymal stroma cells with high osteogenic potency. Injury 2015;46(Suppl 8):S23–32.

[31] Gregory CA, Gunn WG, Peister A, Prockop DJ. An Alizarin red-based assay of mineralization by adherent cells in culture: comparison with cetylpyridinium chloride extraction. Anal Biochem 2004;329:77–84.
[32] Malhan D, Muelke M, Rosch S, Schaefer AB, Merboth F, Weisweiler D, et al. An optimized approach to perform bone histomorphometry. Front Endocrinol (Lausanne) 2018;9:666.
[33] Doube M, Klosowski MM, Arganda-Carreras I, Cordelieres FP, Dougherty RP, Jackson JS, et al. BoneJ: Free and extensible bone image analysis in ImageJ. Bone 2010;47:1076–9.
[34] Kandal S, Ozmen S, Uygur S, Yagci M, Kayhan H, Elmas C, et al. Effects of rat bone marrow-derived mesenchymal stem cells and demineralized bone matrix on cranial bone healing. Ann Plast Surg 2016;77:249–54.
[35] Koc ON, Gerson SL, Cooper BW, Dyhouse SM, Haynesworth SE, Caplan AI, et al. Rapid hematopoietic recovery after coinfusion of autologous-blood stem cells and culture-expanded marrow mesenchymal stem cells in advanced breast cancer patients receiving high-dose chemotherapy. J Clin Oncol 2000;18:307–16.
[36] Koc ON, Day J, Nieder M, Gerson SL, Lazarus HM, Krivit W. Allogeneic mesenchymal stem cell infusion for treatment of metachromatic leukodystrophy (MLD) and Hurler syndrome (MPS-IH). Bone Marrow Transpl 2002;30:215–22.
[37] Horwitz EM, Gordon PL, Koo WK, Marx JC, Neel MD, McNall RY, et al. Isolated allogeneic bone marrow-derived mesenchymal cells engraft and stimulate growth in children with osteogenesis imperfecta: Implications for cell therapy of bone. Proc Natl Acad Sci U S A 2002;99:8932–7.
[38] Le Blanc K, Ringden O. Immunomodulation by mesenchymal stem cells and clinical experience. J Intern Med 2007;262:509–25.
[39] Blanco JF, Villaron EM, Pescador D, da Casa C, Gomez V, Redondo AM, et al. Autologous mesenchymal stromal cells embedded in tricalcium phosphate for posterolateral spinal fusion: results of a prospective phase I/II clinical trial with long-term follow-up. Stem Cell Res Ther 2019;10:63.
[40] Kim SJ, Shin YW, Yang KH, Kim SB, Yoo MJ, Han SK, et al. A multi-center, randomized, clinical study to compare the effect and safety of autologous cultured osteoblast(Ossron) injection to treat fractures. BMC Musculoskelet Disord 2009;10:20.
[41] Berberi A, Al-Nemer F, Hamade E, Noujeim Z, Badran B, Zibara K. Mesenchymal stem cells with osteogenic potential in human maxillary sinus membrane: an in vitro study. Clin Oral Investig 2017;21:1599–609.
[42] Li Q, Yu H, Sun M, Yang P, Hu X, Ao Y, et al. The tissue origin effect of extracellular vesicles on cartilage and bone regeneration. Acta Biomater 2021;125:253–66.
[43] Persson M, Lehenkari PP, Berglin L, Turunen S, Finnila MAJ, Risteli J, et al. Osteogenic differentiation of human mesenchymal stem cells in a 3D woven scaffold. Sci Rep 2018;8:10457.
[44] Zhang G, Chen X, Cheng X, Ma W, Chen C. BMSC seeding in different scaffold incorporation with hyperbaric oxygen treats seawater-immersed bony defect. J Orthop Surg Res 2021;16:249.
[45] Wagner W, Horn P, Castoldi M, Diehlmann A, Bork S, Saffrich R, et al. Replicative senescence of mesenchymal stem cells: a continuous and organized process. PLoS One 2008;3:e2213.
[46] Ksiazek K. A comprehensive review on mesenchymal stem cell growth and senescence. Rejuvenation Res 2009;12:105–16.
[47] Banfi A, Muraglia A, Dozin B, Mastrogiacomo M, Cancedda R, Quarto R. Proliferation kinetics and differentiation potential of ex vivo expanded human bone marrow stromal cells: Implications for their use in cell therapy. Exp Hematol 2000;28:707–15.
[48] Muraglia A, Cancedda R, Quarto R. Clonal mesenchymal progenitors from human bone marrow differentiate in vitro according to a hierarchical model. J Cell Sci 2000;113(Pt 7):1161–6. b.
[49] James S, Fox J, Afsari F, Lee J, Clough S, Knight C, et al. Multiparameter analysis of human bone marrow stromal cells identifies distinct immunomodulatory and differentiation-competent subtypes. Stem Cell Rep 2015;4:1004–15.
[50] Ren J, Wang H, Tran K, Civini S, Jin P, Castiello L, et al. Human bone marrow stromal cell confluence: effects on cell characteristics and methods of assessment. Cytotherapy 2015;17:897–911.
[51] Dominici MLBK, Le Blanc K, Mueller I, Slaper-Cortenbach I, Marini FC, Krause DS, et al. Minimal criteria for defining multipotent mesenchymal stromal cells. The International Society for Cellular Therapy position statement. Cytotherapy 2006;8:315–7.
[52] Bonsignore LA, Anderson JR, Lee Z, Goldberg VM, Greenfield EM. Adherent lipopolysaccharide inhibits the osseointegration of orthopedic implants by impairing osteoblast differentiation. Bone 2013;52:93–101.
[53] Badylak SF, Gilbert TW. Immune response to biologic scaffold materials. In editor. Seminars in immunology. Academic Press; 2008. p. 109–16.
[54] Lee DJ, Diachina S, Lee YT, Zhao L, Zou R, Tang N, et al. Decellularized bone matrix grafts for calvaria regeneration. J Tissue Eng 2016;7:2041731416680306.
[55] Xu K, Kuntz LA, Foehr P, Kuempel K, Wagner A, Tuebel J, et al. Efficient decellularization for tissue engineering of the tendon-bone interface with preservation of biomechanics. PLoS One 2017;12:e0171577.
[56] Gardin C, Ricci S, Ferroni L, Guazzo R, Sbricoli L, De Benedictis G, et al. Decellularization and delipidation protocols of bovine bone and pericardium for bone grafting and guided bone regeneration procedures. PLoS One 2015;10:e0132344.
[57] Smith CA, Richardson SM, Eagle MJ, Rooney P, Board T, Hoyland JA. The use of a novel bone allograft wash process to generate a biocompatible, mechanically stable and osteoinductive biological scaffold for use in bone tissue engineering. J Tissue Eng Regen Med 2015;9:595–604.
[58] Long T, Zhu Z, Awad HA, Schwarz EM, Hilton MJ, Dong Y. The effect of mesenchymal stem cell sheets on structural allograft healing of critical sized femoral defects in mice. Biomaterials 2014;35:2752–9.
[59] Veronesi E, Murgia A, Caselli A, Grisendi G, Piccinno MS, Rasini V, et al. Transportation conditions for prompt use of ex vivo expanded and freshly harvested clinical-grade bone marrow mesenchymal stromal/stem cells for bone regeneration. Tissue Eng Part C Methods 2014;20:239–51.
[60] Mebarki M, Coquelin L, Layrolle P, Battaglia S, Tossou M, Hernigou P, et al. Enhanced human bone marrow mesenchymal stromal cell adhesion on scaffolds promotes cell survival and bone formation. Acta Biomater 2017;59:94–107.
[61] Hashimoto Y, Funamoto S, Kimura T, Nam K, Fujisato T, Kishida A. The effect of decellularized bone/bone marrow produced by high-hydrostatic pressurization on the osteogenic differentiation of mesenchymal stem cells. Biomaterials 2011;32:7060–7.
[62] Leotot J, Coquelin L, Bodivit G, Bierling P, Hernigou P, Rouard H, et al. Platelet lysate coating on scaffolds directly and indirectly enhances cell migration, improving bone and blood vessel formation. Acta Biomater 2013;9:6630–40.
[63] Qi H, Ye Z, Ren H, Chen N, Zeng Q, Wu X, et al. Bioactivity assessment of PLLA/PCL/HAP electrospun nanofibrous scaffolds for bone tissue engineering. Life Sci 2016;148:139–44.
[64] Lu W, Gao B, Fan J, Cheng P, Hu Y, Jie Q, et al. Mesenchymal progenitors derived from different locations in long bones display diverse characteristics. Stem Cells Int 2019;2019:5037578.
[65] Tanikake Y, Akahane M, Furukawa A, Tohma Y, Inagaki Y, Kira T, et al. Calcium concentration in culture medium as a nondestructive and rapid marker of osteogenesis. Cell Transplant 2017;26:1067–76.
[66] Wang J, Yin Q, Gu S, Wu Y, Rui Y. Induced membrane technique in the treatment of infectious bone defect: a clinical analysis. Orthop Traumatol Surg Res 2019;105:535–9.
[67] Robey PG, Riminucci M. Skeletal stem cells: Tissue-specific stem/progenitor cells of cartilage, bone, stroma, and marrow adipocytes. In editor. Principles Bone Biol 2020:45–71.
[68] Cheng L, Li Y, Xia Q, Meng M, Ye Z, Tang Z, et al. Enamel matrix derivative (EMD) enhances the osteogenic differentiation of bone marrow mesenchymal stem cells (BMSCs). Bioengineered 2021;12:7033–45.